PROCEEDINGS OF SCIENCE

# Measurement of gamma-ray emission from neutron-$^{16}$O reactions with an 80 MeV quasi-mono energetic neutron beam

**Yosuke ASHIDA**[*†]
*kyoto University (Japan)*
*E-mail:* assy@scphys.kyoto-u.ac.jp

Precise knowledge of neutrino neutral current elastic interaction on oxygen is important to improve the sensitivity in search for supernova relic neutrinos at Super-Kamiokande. While the measurement of the interaction cross section is successfully conducted at the T2K experiment using as signal gamma-rays emitted from excited nuclei, a large systematic error remains since the current model, which is used for the predictions of gamma-ray emission through nuclear reactions following the primary neutrino interaction, is not optimal. To reduce the systematic uncertainty, the measurement of gamma-ray production from neutron-oxygen reactions is carried out using an 80 MeV quasi-mono energetic neutron beam. In the experiment, several gamma-ray peaks from the reactions of oxygen nuclei with fast neutrons are observed. In addition, neutron flux and background measurements are also conducted for the cross section estimation. Using the data, the production cross section of 6.13 MeV gamma-ray, which is important in the T2K measurement, is estimated. Finally, future prospects are also reported.

*The 19th International Workshop on Neutrinos from Accelerators (NUFACT2017)*
*25-30th, September, 2017*
*Uppsala University, Uppsala, Sweden*

[*]Speaker.
[†]The RCNP-E487 Collaboration





PoS(NuFact2017)077

## 1. Introduction

Precise knowledge of neutrino neutral current elastic (NCE) scattering is important for several physics searches at Super-Kamiokande (SK) [1]. For example, the NCE interaction of atmospheric neutrinos is one of the main background sources in search for supernova relic neutrinos [2, 3]. In the T2K experiment [4], the NCE interaction cross section is measured using the gamma-rays emitted from the nuclei excited by primary neutrino interactions as signal [5]. The systematic error in the measurement is large mainly due to the uncertainties of the implemented nuclear reaction model GCALOR [6]. In the T2K neutrino energy region (sub-GeV), the NCE interaction dominantly involves one nucleon knock-out (conventionally called NC quasi-elastic; NCQE [7]) and those nucleons, especially neutrons, would cause additional nuclear reactions within the detector leading to further gamma-ray emission. The kinetic energy of knocked-out nucleons ranges from 20 to several hundred MeV. The model that describes these secondary gamma-ray emission is not optimal, and a large uncertainty remains. Currently 13% of the total 20% uncertainty in the NCE measurement is attributed to this model. There is little experimental studies on the gamma-ray production cross section on oxygen using fast neutrons with more than 20 MeV of kinetic energy, while several theoretical models exist. To select or create an appropriate model based on real data, we conduct an experiment using an 80 MeV quasi-mono energetic fast neutron beam.

## 2. Experimental details

The experiment was carried out at the neutron time-of-flight beam line of Osaka University's Research Center for Nucler Physics (RCNP). Figure 1 shows a schematic drawing of the facility and our setup.

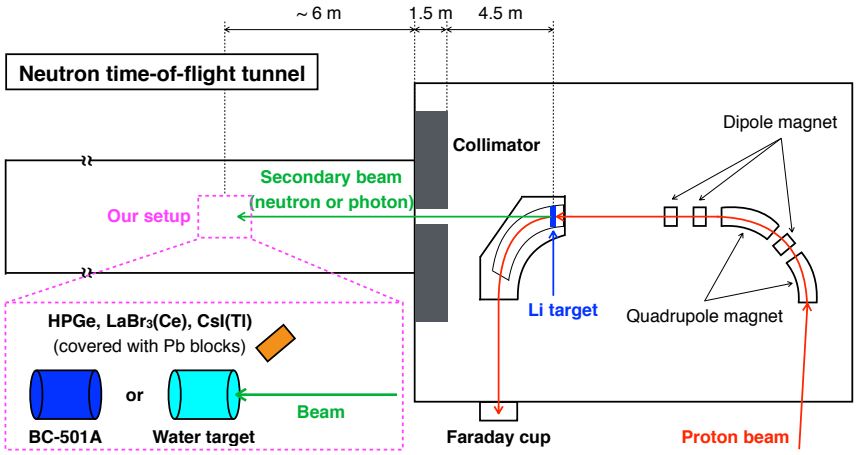


**Figure 1:** Schematic drawing of the RCNP facility and experimental setup.

Protons are accelerated to a kinetic energy of 80 MeV by two cyclotrons, then directed to the Li target with 10 mm thickness. Through $^{7}\mathrm{Li}(\mathrm{p},\mathrm{n})^{8}\mathrm{Be}$ reaction, an almost mono energetic neutron beam is obtained. The beam collimator made of iron and concrete is placed behind the Li

target and the magnetic field is applied to bend charged particles so that only neutrons and gamma-rays are coming into the neutron beam line. During the beam test, the energy of protons is kept $80 \pm 0.6$ MeV. Each proton beam bunch has 200 ps width and the bunch period is 562.5 ns.

A cylindrical-shaped acrylic container filled with water, which has the size of 20 cm diameter and 26 cm long and thickness of 1 cm, is placed on the beam axis 12 m away from the Li target. For the main gamma-ray measurement, two types of detectors, a $LaBr_3(Ce)$ scintillator and an HPGe detector, are placed upstream of this water target where neutron scatter is considered to be relatively small. The neutron background here is also measured by a CsI(Tl) scintillator placed near the gamma-ray detectors. These detectors are covered with lead blocks to reduce large background in the beam line. These measurements are carried out both with and without the water to estimate the contribution only from water component. In no-water runs, just the acrylic vessel is placed. To obtain the cross section, neutron flux measurement is separately carried out using an organic liquid scintillator (BC-501A) replacing the water target on-axis. The $LaBr_3(Ce)$ and the BC-501A are read-out by VME 12-bit QDC (CAEN V792) and 12-bit TDC (CAEN V775), the CsI(Tl) by 12-bit 250 MHz Flash-ADC (CAEN DT5725), and HPGe by MCA (Kromek K102). In all the measurements, the proton current is measured using a Faraday cup implemented with the facility and read-out by a counter (ORTEC 439). The results are normalized with proton current in the offline analysis. For the energy calibration of $LaBr_3(Ce)$, HPGe, and CsI(Tl), several types of gamma-ray sources and gamma-ray peaks from thermal neutron captures that are observed during the beam irradiation are used. The detectors are well calibrated up to 8 MeV. As for the BC-501A calibration that is needed for the detection efficiency calculation, electrons of known energy arising from Compton scattering by a gamma-ray source are used.

## 3. Analysis results

### 3.1 Neutron flux

The raw data contains charge information with different integration regions (total charge and tail charge) and time information. The first is used to extract neutron events based on Pulse Shape Discrimination (PSD) technique and the second is for the reconstruction of neutron kinetic energy. The left panel of Figure 2 shows the PSD parameter (the ratio of tail charge to total charge) versus total charge. Clear separation between gamma-ray and neutron events is observed. As for neutron-induced events, several lines are seen that are contributed from different charged particles produced through reactions such as $(n,p)$ or $(n,\alpha)$. Using the difference, PSD cut is applied to extract neutron events. The saturated events, whose energy is larger than the QDC dynamic range and the PSD cannot be applied, are assumed to be neutrons and systematic error is estimated for this assumption. The right panel of Figure 2 shows the time-of-flight (TOF) distriution. Black refers to all events and blue (red) to neutron (gamma-ray) events after PSD cut. Here the time walk effect is corrected. Two peaks are seen here, and the right sharp peak is from gamma-rays emitted via p-Li reactions (called prompt-$\gamma$) and the left one mainly from neutrons. The prompt-$\gamma$ peak is used for the zero-point of time to determine the neutron kinetic energy.

The detection efficiency is calculated using the Monte Carlo code SCINFUL-QMD [8, 9]. Inputs to the code are the detector type, size, geometry, and detector threshold in $MeV_{ee}$. The

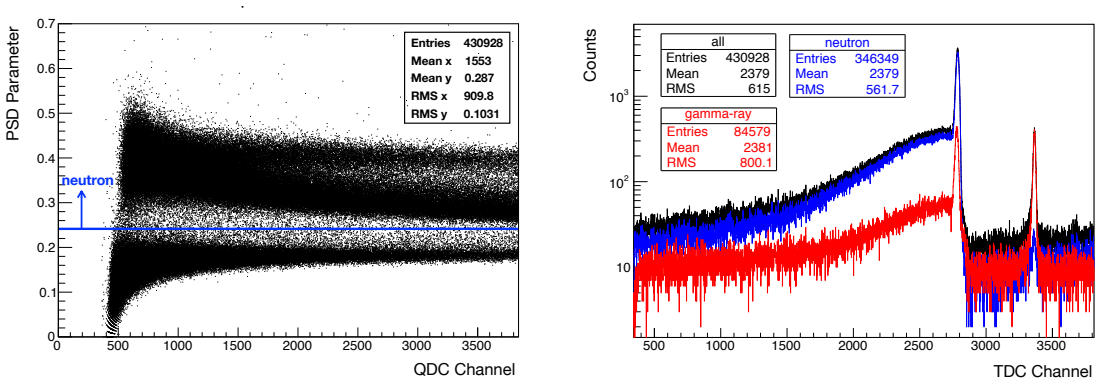


**Figure 2:** The PSD distribution (left) and TOF distribution (right) of the BC-501A detector.

calculation is done up to neutron kinetic energy 99 MeV with the bin of 1 MeV. The results are shown in the left panel of Figure 3. Neutron flux is obtained by dividing each bin of kinetic energy distribution with detection efficiency. The right panel of Figure 3 shows the flux result after normalization with beam current and detector acceptance. It peaks at around 77 MeV and has long tail. For the cross section estimation, only peak region is used because tail region contains not just slow neutrons but also scattered fast neutrons (“fake events").

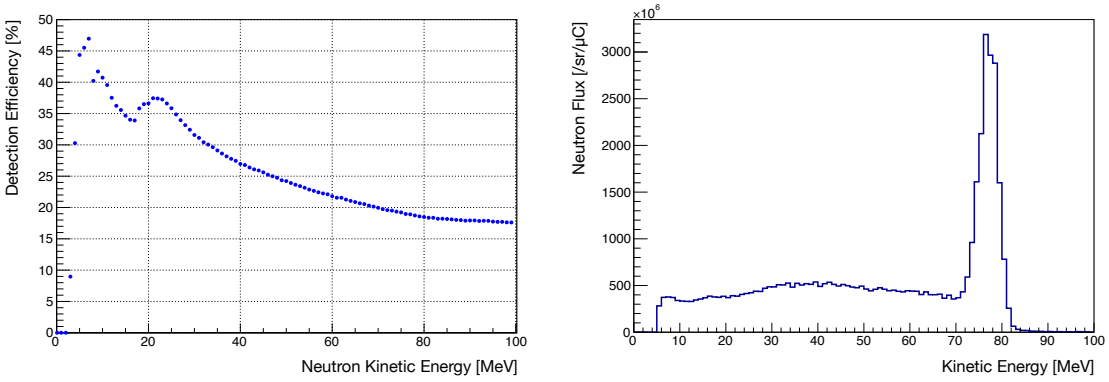


**Figure 3:** The neutron detection efficiency of the BC-501A detector calculated by SCINFUL-QMD (left) and the reconstructed flux (right).

The statistical error is estimated to be 0.5% in the peak region. The dominant systematic error (10%) comes from the SCINFUL-QMD physics model [10]. The next leading systematic uncertainty is the beam condition. In the beam test, we measured flux several times and the fluctuation of the results are considered as systematic error (3.4%). The error related to neutron selection (PSD and overflow events) is 2.2%. The other sources such as former bunch or environmental contamination are negligible. Totally, 10.9% is estimated as uncertainty in this measurement.

### 3.2 Gamma-ray production

Several peaks are observed with gamma-ray detectors that are considered to originate from neutron-$^{16}$O reactions. The results from HPGe detector with MCA read-out is shown in Figure 4. The spectrum with red color corresponds to the measurement with the water filled target, and one

with blue does without water. The spectra are normalized with the proton beam current and water target acceptance. Here S.E. refers to the single escape peak and D.E. the double escape peak. Several peaks from neutron-nucleus reactions are observed: hydrogen, carbon, nitrogen, oxygen, and iron. These peaks are observed also in a $LaBr_3(Ce)$ spectrum but with more ambiguous due to worse energy resolution. We have time information for the $LaBr_3(Ce)$, then only peak neutron region is extracted when the cross section is calculated.

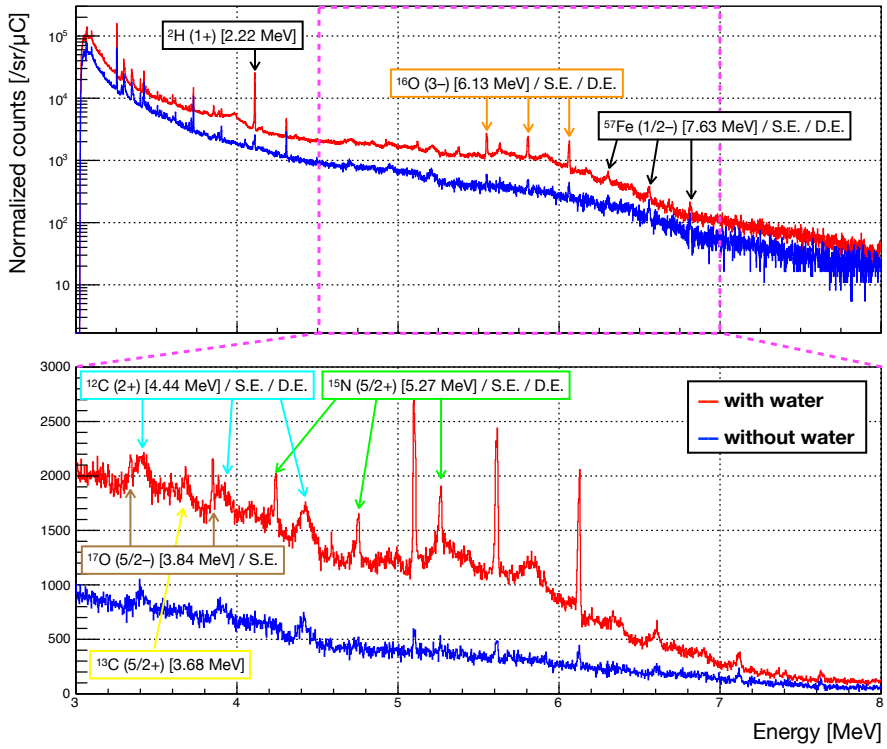


**Figure 4:** Energy spectra of HPGe detector (MCA read-out). Red is the result with water, and blue without water. Both are normalized with the incident proton beam current and water target acceptance.

To identify the physics processes behind the observed gamma-ray peaks, we use two information as clues in addition to energy. One is the doppler effect that makes the peak width larger if the parent nucleus is relatively light. From this 4.44 and 3.68 MeV peaks are considered to be from excited carbon. The other is the fact that it is more probable to decay into the state with large energy gap from the original excited state or with large angular momentum in the decay with particle emission. For example, in the decay of $^{16}O(3^-)$ into $^{15}N+p$, the dominant state of residual nitrogen is $^{15}N(\frac{5}{2}^+)$. The dominant process is considered to be $^{16}O(n,n')^{16}O^*$ in which the residual oxygen is in the state with spin-parity $3^-$. The 6.13 MeV gamma-ray is emitted through the transition from the $^{16}O^*(3^-)$ to the ground state. If the residual state is higher than the particle emission threshold, the de-excitation is attained with the emission of a particle such as proton, neutron, or alpha. As for the case of $^{16}O$, the threshold for alpha emission is lowest (7.16 MeV), that for proton is 12.13 MeV, and that for neutron is 15.66 MeV. In the E487 experiment, only the gamma-rays from excited nitrogen and carbon are observed through the processes such as $^{16}O^* \rightarrow^{15} N^*(\frac{5}{2}^+)+p$ then $^{15}N^* \rightarrow^{15} N+\gamma(5.27\ MeV)$ and

$^{16}O^* \rightarrow ^{12}C^*(2^+) + \alpha$ then $^{12}C^* \rightarrow ^{15}N + \gamma(4.44\ \mathrm{MeV})$. This is reasonable considering the order of particle thresholds. Note that in direct knock-out processes the dominant gamma-ray is reported to be 6.32 MeV from $^{15}N(\frac{3}{2}^-)$ [11, 12]. The 3.84 MeV peak is considered to be from $^{17}O(\frac{5}{2}^-)$ that is created through the neutron capture by $^{16}O$. The 3.68 MeV gamma-ray is though to be emitted from $^{12}C(\frac{5}{2}^+)$. This is produced through the reaction $^{16}O(n,\alpha)^{13}C^*$. In this proceedings, the gamma-ray production cross section for 6.13 MeV is estimated since it is the strongest peak after the peak neutron cut.

### 3.3 Background estimation

The contribution of the acrylic container is subtracted by using data from the measurement with no water filled as shown in Figure 4.

Even though the gamma-ray detector is placed at upstream position and covered with lead blocks, scattered neutron background may exist. To estimate the contamination amount, the CsI(Tl) PSD method [13] is used. Using the PSD and the time information, we estimate the neutron background contamination around the signal region to be 2%.

After the background subtraction of the acrylic container and scattered neutrons, the continuous component remains. This is estimated by using side-bands of the signal peak and subtracted. The signal counting window is determined by the energy resolution at the peak, and systematic uncertainty related to this is estimated by changing window based on resolution error.

### 3.4 Cross section estimation

The gamma-ray production cross section ($\sigma_\gamma$) is estimated as follows:

$$\sigma_\gamma = \frac{N_{\mathrm{sig}} - N_{\mathrm{bkg}}}{\phi_n \varepsilon_\gamma T}, \tag{3.1}$$

where $N_{\mathrm{sig}}$ and $N_{\mathrm{bkg}}$ represent the normalized number of all and background events in the signal counting window $[/\mathrm{sr}/\mu\mathrm{C}]$, $\phi_n$ is the normalized neutron flux $[/\mathrm{sr}/\mu\mathrm{C}]$, $\varepsilon_\gamma$ is the gamma-ray detection efficiency, and $T$ is the number of target nuclei ($^{16}O$) per area $[/\mathrm{cm}^2]$. The detection efficiency is calculated by Geant4 simulation [14] for the signal window. The estimated cross section of 6.13 MeV gamma-ray production via 77 MeV neutron scattering on $^{16}O$ is 6.1 mb (preliminary). The statistical uncertainty is 2.0%. The largest systematic uncertainty comes from the continuous background estimation. Due to insufficient resolution of the $LaBr_3(Ce)$ detector, the side-band estimation gives 23.0% uncertainty. The other sources related to background estimation is small enough. The next leading uncertainty is neutron flux measurement (10.9%). Other sources are gamma-ray detection efficiency (1.7%) and target material size (0.4%). The total 25.6% uncertainty is estimated preliminarily.

## 4. Summary and prospects

In this proceedings, the E487 experiment conducted using an 80 MeV neutron beam at RCNP and its preliminary analysis results are reported. Neutron flux is measured with the BC-501A using

the TOF and PSD analysis. Several gamma-ray peaks through excited oxygen states are observed both with the HPGe and $LaBr_3(Ce)$ detector. The estimation of scattered neutron background is also achieved with CsI(Tl) pulse shape analysis. Using them a preliminary cross section value for 6.13 MeV gamma-ray production is calculated to be $\sigma_{\gamma(6.13\ \mathrm{MeV})} = 6.1 \pm 0.1(stat.) \pm 1.6(syst.)$ mb.

Additional measurements are planned with the basically similar methods but with different energies (already approved by RCNP officially as E525). Two beam energies will be used: 1) 30 MeV, because the physics reaction may change drastically near the oxygen Fermi surface (27 MeV) and the peak neutron energy after the NCQE is nearly the Fermi surface, 2) 246 MeV, so to measure at high energy avoiding large background from gamma-rays by neutral pion decays, since the pion production threshold for the fixed target is about 250 MeV. Using all results, the modification of the T2K model will be performed.

## Acknowledgment

We thank the RCNP for approving our beam test and supplying a beam. This work was partially supported by MEXT KAKENHI Grant Number 17J06141, 26400292, and 25105002.

## References

[1] K. Fukuda *et al*., Nucl. Instr. Meth. Phys. Res. A, 501 (2003)

[2] K. Bays *et al*. (Super-Kamiokande Collaboration), Phys. Rev. D 85, 052007 (2012)

[3] H. Zhang *et al*. (Super-Kamiokande Collaboration), Astropart. Phys. 60, 41 (2015)

[4] K. Abe *et al*. (T2K Collaboration), Nucl. Instr. Meth. Phys. Res. A 659 (2011)

[5] K. Abe *et al*. (T2K Collaboration), Phys. Rev. D 90, 072012 (2014)

[6] C. Zeitnitz and T. A. Gabriel, Proceedings of the International Conference on Monte Carlo Simulation in High Energy and Nuclear Physics (MC93) (1993)

[7] Arthur M. Ankowski *et al*., Phys, Rev. Lett. 108, 052505 (2012)

[8] D. Satoh *et al*., JAEA-DATA/CODE 2006-023 (2006)

[9] T. Kajimoto *et al*., Nucl Inst. Meth. Phys. Res. A 665 (2011)

[10] Y. Iwamoto *et al*., Nucl. Inst. and Meth. Phys. Res. A 804 (2015)

[11] H. Ejiri, Phys. Rev. C 48, 1442 (1993)

[12] M. Leuschner *et al*., Phys. Rev. C 49, 955 (1994)

[13] Y. Ashida *et al*., Prog. Theor. Exp. Phys. 043H01 (2018)

[14] S. Agostinelli *et al*., Nucl. Inst. and Meth. Phys. Res. A 506 (2003)